Volume 50 | Number 49 | 21 June 2014 | Pages 6411–6544

ChemComm

Chemical Communications

www.rsc.org/chemcomm

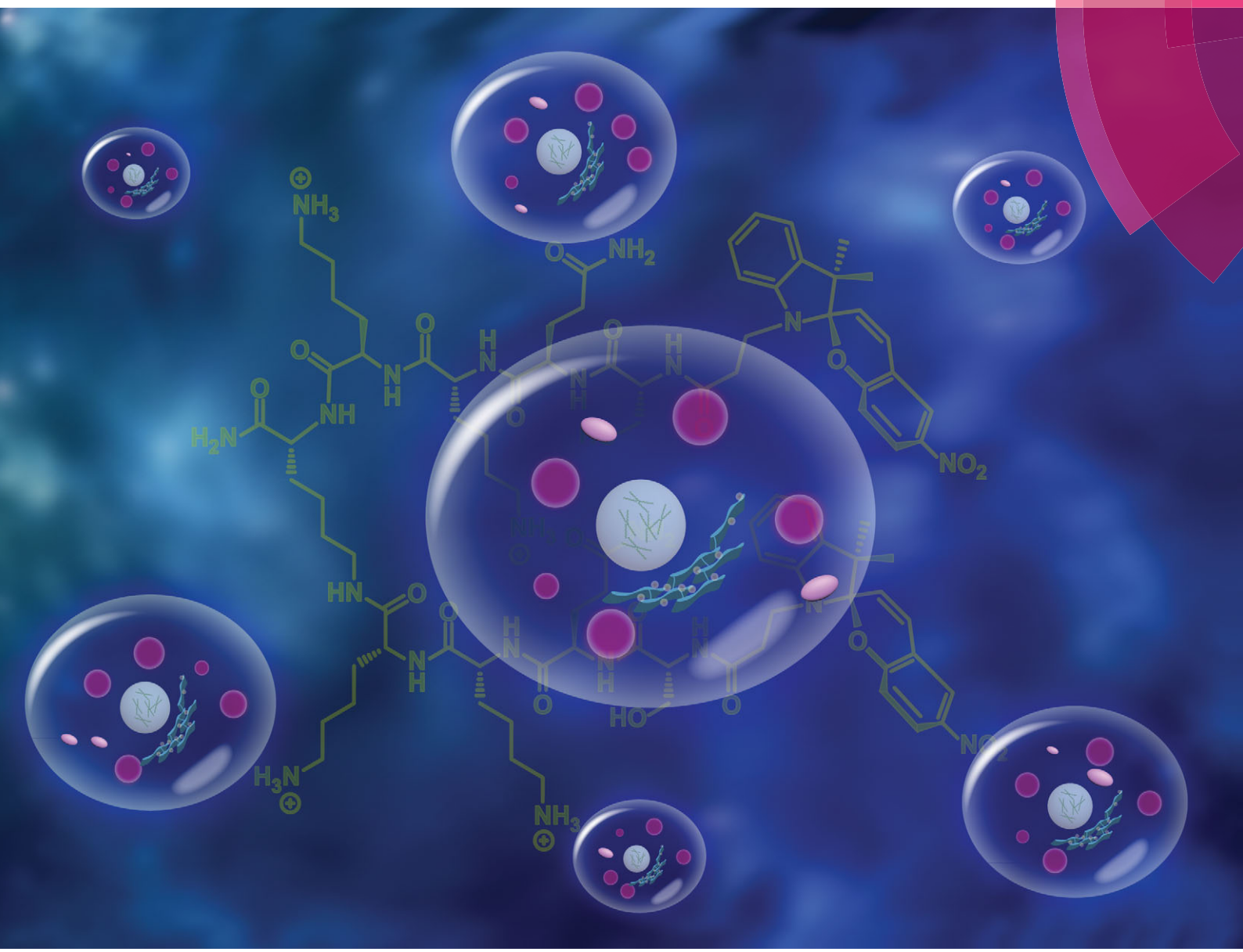

ISSN 1359-7345

ROYAL SOCIETY OF CHEMISTRY

COMMUNICATION

Junchen Wu, He Tian *et al.*

A switchable peptide sensor for real-time lysosomal tracking

ChemComm

COMMUNICATION

View Article Online
View Journal | View Issue

A switchable peptide sensor for real-time lysosomal tracking†

Cite this: *Chem. Commun.*, 2014, 50, 6443

Received 25th January 2014,
Accepted 27th March 2014

DOI: 10.1039/c4cc00670d

www.rsc.org/chemcomm

Lei Chen,[a] Junchen Wu,*[a] Carsten Schmuck[b] and He Tian*[a]

A bis-spiropyran functionalized peptide 1, which exhibits good cell-permeability, excellent biocompatibility and low cytotoxicity, has been developed for reversible and real-time lysosomal tracking.

Lysosomes, as membrane-bound organelles, contain a large variety of hydrolytic enzymes and secretory proteins that are active at an acidic luminal pH range (~4.0 to 5.5).[1] Lysosomes are not only serving as the terminal degradative compartment of live cells, but are also involved in many physiological processes including metabolism, intracellular transport, and cell membrane recycling as well as apoptosis.[2] However, lysosomal malfunctions can lead to different pathophysiological conditions,[3] especially to cancer-related diseases.[4] Thus, effective strategies to visualize lysosomes of cancer cells are of significant interest in preventing or treating tumor invasion and metastasis and will pave the way for lysosome-related disease diagnosis and therapy.

Very recently, several efforts have been devoted to the development of fluorescent sensors employed to study lysosomal functions in live cells, which include polymers,[5] nanoparticles,[6] modified quantum dots,[7] and macromolecules, such as dextran labeled with a fluorophore.[8] Although these sensors can be exploited to track the intracellular lysosomes efficiently, they also exhibit the following limitations: (i) it is difficult to target them on specific lysosomal lumen with high spatial and temporal resolution; (ii) they often suffer from poor solubility in water and display poor biocompatibility; and (iii) they show irreversible switching cycles limiting the span of time-lapse imaging. Considering these difficulties, it is imperative to develop a new sensor to track lysosomes with good solubility, high efficiency and excellent biocompatibility. In addition, sensors capable of reversibly monitoring lysosomal imaging are also desirable. This ideal probe, however, has rarely been reported in the field of lysosomes.

Until now, spiropyran derivatives were widely applied from data storage[9] to optical switching,[10] chemical sensing,[11] molecular machines[12] and logic gate,[13] based on the reversible structural isomerization from a colorless spiro-form (spiropyran, **SP**) to a colored open-form (merocyanine, **Mc**) by UV/Vis light illumination. However, a pH-active spiropyran based sensor used to track intracellular lysosomes has been rarely explored. Moreover, it should be noted that the intrinsic photoswitchable property of spiropyran could be achieved by either pH or Vis-light realizing reversible lysosomal tracking. Therefore, we expected to employ a spiropyran fluorophore with a structurally simpler lysine-rich cationic peptide to be used for lysosomal tracking. This photoswitch would allow us to track and recognize lysosomes with high signal-to-noise ratio upon spectroscopic changes being imposed by pH-changes in aqueous solution.

In this work, a bis-spiropyran functionalized peptide **1** (Scheme 1a) was specifically designed in anticipation of the tracking of the lysosome upon the protonation of spiropyran moieties as well as the electrostatic interaction of positively charged lysine residues with negatively charged lysosomal membranes. This peptide has been proved to serve as a pH and light dual-responsive photoswitch, in which the pH-induced ring opening process was thoroughly studied. Moreover, **1** was well employed for reversible lysosomal tracking within live cells. Peptide **1** was synthesized using a microwave-assisted solid-phase peptide method that is commonly used for peptide-based biosensors,[14] which was isolated by preparative HPLC on a reversed-phase C-18 column in 99% purity and 25% yield, respectively (ESI†).

To identify the best pH-responsive conditions, the spectroscopic studies of **1** were examined by UV/Vis absorption and fluorescence spectroscopy in Tris-HCl buffer solutions (TBS) in a pH range from 2.0 to 10.0. Below pH 2, **1** shows a sharp absorption band at 410 nm and relatively weak fluorescence emission at 623 nm (Fig. S1a and b, ESI†). The absorption band at 410 nm is attributed to the protonation of the phenolate anion of the merocyanine units (**McH**$^+$), which is consistent with previous research.[15] In contrast, the fluorescence

[a] *Key Labs for Advanced Materials and Institute of Fine Chemicals, East China University of Science and Technology, Shanghai 200237, China. E-mail: jcwu@ecust.edu.cn, tianhe@ecust.edu.cn; Fax: +86 21 6425 2288; Tel: +86 21 6425 3674*

[b] *Institute for Organic Chemistry, University of Duisburg-Essen, Universitätsstraße 7, 45117 Essen, Germany*

† Electronic supplementary information (ESI) available: Experimental details and more spectroscopic data. See DOI: 10.1039/c4cc00670d

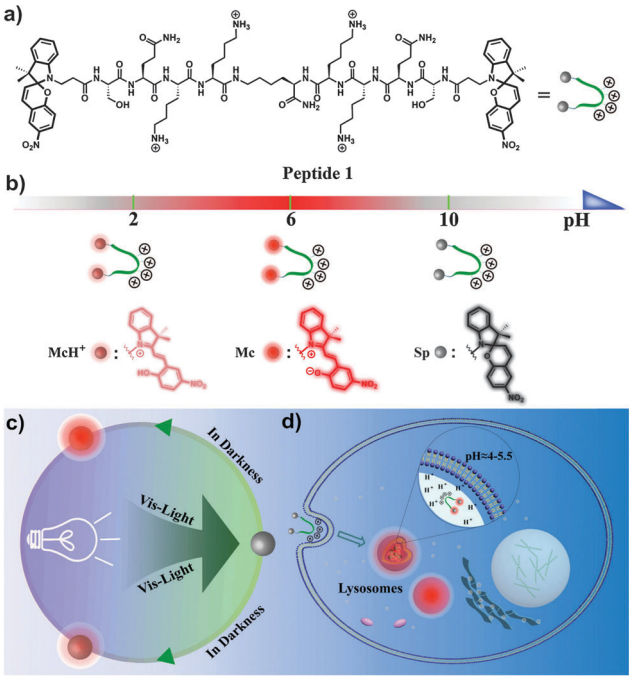

Scheme 1 (a) Molecular structure of peptide **1**; (b) the coordinate represents the states of sensor at different pH values, purple sphere: protonated merocyanine (**McH$^+$**), red sphere: normal merocyanine (**Mc**), and gray sphere: spiropyran at a ring-closed state (**Sp**). (c) The photo-physical process of **1** at the corresponding pH; (d) the cartoon image shows the work principle of peptide **1** for live cell lines.

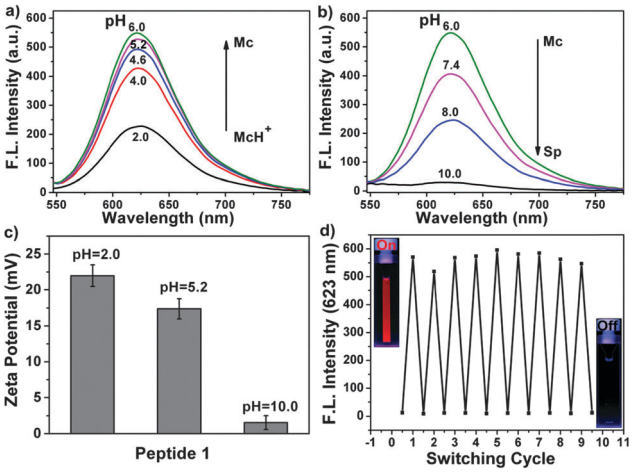

Fig. 1 (a) and (b) Fluorescence spectra of peptide **1** (50 μM) measured at different pH values in TBS (0.05 M Tris, 0.05 M NaCl, 20 °C) for 12 h (arrows show the direction of intensity increase from 2.0 to 6.0 and intensity decrease from 6.0 to 10.0, respectively); (c) zeta potentials of peptide **1** measured at different pHs (pH = 2.0, 5.2 and 10.0, respectively), results were presented as mean ± SD (n = 3). (d) Sequential fluorescence switching cycles of peptide **1** controlled by Vis-light illumination for *ca.* 10 min and placed in darkness for 12 h in TBS (pH 5.2, 0.05 M Tris, 0.05 M NaCl, 20 °C), inset: fluorescence images (UV light, 365 nm).

spectral changes of **1** at various pH values (4–6) are shown in Fig. 1a. Increasing the pH value gives rise to higher fluorescence intensity at 623 nm (Fig. S2b–S5b, ESI†), while the absorption band of **1** exhibits a bathochromic shift from 410 nm to 514 nm concomitantly (Fig. S2a–S5a, ESI†), a representative absorption of **Mc**.[15] As seen in Fig. 1a, the relative fluorescence intensities increased by approximately 3-fold from pH 2 to 6. Indeed, it is noteworthy that **1** exhibits strong increase in the fluorescence intensities in the pH range of *ca.* 4–6, which covers both normal and abnormal lysosome pH making **1** a promising fluorescent indicator (Scheme 1b) for lysosome. However, at pH ≥ 10.0, neither UV-Vis absorption nor fluorescence emission could be observed (Fig. 1b and Fig. S8a and b, ESI†), suggesting the presence of the ring-closed state (**SP**). Besides, zeta potential measurements at specific pH values (pH 2.0, 5.2 and 10.0) indicated a decrease of surface-charge of **1** with the increase of pH values (zeta potential: 21.97 ± 1.52 mV, 17.38 ± 1.41 mV and 1.55 ± 0.97 mV at pHs 2.0, 5.2 and 10.0, respectively, Fig. 1c), which further confirmed that **1** exhibited three different states (**McH$^+$**, **Mc** and **Sp**) at the pH range from 2 to 10. Moreover, we were excited that, as evident in Fig. 1d (pH 5.2), the photo switching of the fluorescence could be repeated many times without any apparent "fatigue" effects. The reversible switching processes could also be cycled under the pH range of pH 4–6 (details are not given). In contrast, the ring opening processes were also measured by UV light irradiation (Fig. S1c–S8c, S1d–S8d, ESI†). Interestingly, upon irradiation with UV light (365 nm), little or no changes of absorption and fluorescence were detected in contrast to the behaviour in darkness. This confirms that **1** effectively realizes the ring-opening process in aqueous solution with the concomitant occurrence of red luminescence by pH-changes rather than UV light irradiation. Moreover, with the irradiation of Vis-light, the ring-closing process of **1** occurs (Scheme 1c). To determine the physical parameters of **1** at various pH values from 2.0 to 10.0, the fluorescence quantum yield (Φ) was measured, providing a maximum of 3.1% with a lifetime for a single-exponential decay of 0.38 ns at pH 4–6 (Table S2, ESI†).

On the basis of the above results, we evaluated whether **1** could be efficiently taken up by cancer cells. After incubating live A549 cells with **1** for 1 h, an intense red luminescence was detected in the cytoplasmic region, while no luminescence in the nucleus was observed (Scheme 1d, Fig. 2 and Fig. S9 and S10, ESI†). We could deduce that the red signals most likely came from the acidic organelles (the intracellular lysosomes). To confirm these results, a colocalization experiment of **1** with LysoTracker Green DND-26 (LTG) was performed. As shown in Fig. 2, cell images confirmed that the red and green signals from **1** (Fig. 2a) and LTG (Fig. 2b) originated from approximately the same cell region. The overlay images revealed that **1** mainly accumulates in the acidic lysosomes instead of the nucleus (Fig. 2d and e). In addition, amplified imaging of A549 cells shown in Fig. 2g and cross-sectional analysis (quantification of the luminescence intensity profile of **1** and LTG along the white line in image 2g, Fig. 2h) indicated that the luminescence indeed mainly stems from the lysosomes (spot 2) rather than the nucleus (spot 3). These facts suggest that **1** showed good specificity toward lysosomes and could act as a potential candidate of a lysosomal tracking agent.

Subsequently, exploration of **1** as a switchable sensor to track lysosomes was carried out by incubating A549 cells. Firstly, a time course ring-opening process of **1** was conducted within cells.

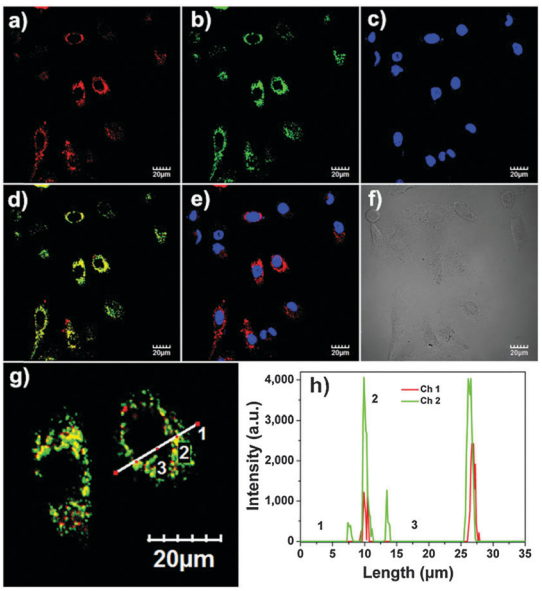

Fig. 2 Colocalization experiments using peptide **1**, LysoTracker Green DND-26 (LTG) and Hoechst 33258 in A549 cells. Cells were stained with (a) 10 μM peptide **1** (channel 1: excitation: 515 nm, emission collected: 600–650 nm), (b) 0.1 μM LTG (channel 2: excitation: 488 nm, emission collected: 500–550 nm) and (c) 10 μg mL^{-1} Hoechst 33258 (channel 3: excitation: 405 nm, emission collected: 420–470 nm); (d) overlay of (a) and (b); (e) overlay of (a) and (c); (f) overlay of (a) and bright-field; (g) partially enlarged image of (d) (cross-sectional analysis along the white line in regions of 1, 2 and 3); (h) intensity profile of regions of interest across one A549 cell.

After treatment with visible light for *ca.* 5 min, no obvious fluorescence was detected by laser confocal microscopy, which suggested that **1** was present in the ring-closed form upon illumination. Then, the images were recorded as time elapsed. Interestingly, the A549 cells were highlighted with red fluorescence and became increasingly brighter as the time elapsed. After the cells being kept in darkness for *ca.* 15 min, the red fluorescence of **1** almost revived (Fig. 3a–f). After that, the photoswitchable lysosomal tracking was performed using processes of irradiation of Vis-light for *ca.* 5 min and keeping in darkness for *ca.* 15 min successively. As shown in Fig. 3g and h and Fig. S11 (ESI†), the reversible off–on fluorescence imaging of targeted cells could be repeated at least eight times within cells with little photobleaching, which was attributed to the acidic atmosphere induced ring-opening instead of an UV light induced process. In this case, the harm to live cells caused by UV-light can be readily avoided. Furthermore, the time-lapse ring-opening process made **1** a potential candidate for real-time dynamic monitoring of lysosome.

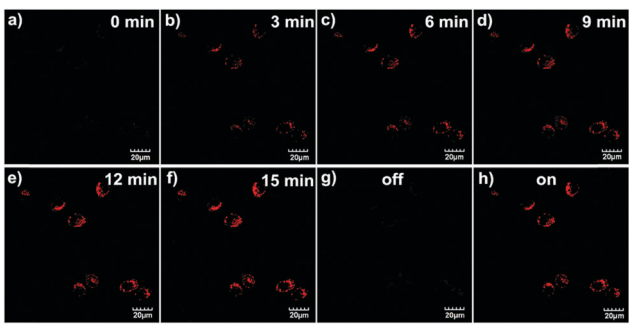

Fig. 3 (a)–(f) Time dependence of the fluorescence revival process of **1** from 0 to 15 min in darkness (without UV irradiation), the process took place after irradiation of visible light for *ca.* 5 min and kept in darkness as time elapsed; images of switching process of **1** within lysosomes in A549 cell lines; (g) switch-off state: irradiation of Vis-light for *ca.* 5 min erases the red fluorescence; (h) switch-on state: placed in darkness for *ca.* 15 min revives the red fluorescence.

For potential applications, the cell toxicity of **1** towards A549 and HeLa cell lines was measured using a standard 3-(4,5-dimethyl-2-thiazolyl)-2,5-diphenyltetrazolium bromide (MTT) assay. As shown in Fig. S12 (ESI†), upon incubation with a significantly higher concentration of 40 μM for 12 h, the cell viabilities were still nearly 85%, indicating that **1** showed low cytotoxicity towards live cells. This bodes well for the utility of this peptide probe, particularly in live cell imaging applications for lysosomal tracking. To further explore the cellular entry pathway of **1**, staining with **1** was investigated under conditions of different temperatures. At 4 °C, active cellular uptake of **1** by A549 cells was blocked (Fig. S9a–c, ESI†). In contrast, at 37 °C, uptake of **1** into the cells and subsequent staining of lysosomes was clearly observed (Fig. S9d–f, ESI†), suggesting that cellular uptake of **1** occurred in an energy-dependent fashion, most likely *via* endocytosis. Hence, peptide **1** was efficiently taken up by cells, which was largely attributed to the specific lysine-rich sequence and the excellent water solubility.

In summary, we have demonstrated that peptide **1** with spiropyran units can be used as a switchable sensor to reversibly track lysosomes in live cell lines in real-time. Upon accumulation in intracellular lysosomes, the low pH of lysosomal lumen promotes the ring-opening of the spiropyran units, which, as a result, makes it possible for **1** to serve as a lysosomal sensor. Moreover, as the process can be tuned by pH and visible light, it enables us to reversibly label lysosomes, which has been realized here for the first time to the best of our knowledge. Furthermore, as peptide **1** does not possess any general cytotoxicity, it might be of interest for application in tumor diagnosis and therapy.

We thank the National Basic Research 973 Program (2013CB733700) and the Fundamental Research Funds for the Central Universities (WJ1213007), the innovation program of shanghai municipal education commission (J100-2-13104), the Program of Shanghai Pujiang (K100-2-1275) for financial support.

Notes and references

1 (*a*) J. Zhou, S. H. Tan, V. Nicolas, C. Bauvy, N. D. Yang, J. B. Zhang, Y. Xue, P. Codogno and H. M. Shen, *Cell Res.*, 2013, **23**, 508; (*b*) H. B. Yu, Y. Xiao and L. J. Jin, *J. Am. Chem. Soc.*, 2012, **134**, 17486; (*c*) H. Zhu, J. L. Fan, Q. L. Xu, H. L. Li, J. Y. Wang, P. Gao and X. J. Peng, *Chem. Commun.*, 2012, **48**, 11766.
2 (*a*) F. K. Fan, S. Nie, D. M. Yang, M. J. Luo, H. Shi and Y. H. Zhang, *Bioconjugate Chem.*, 2012, **23**, 1309; (*b*) C. Settembre, A. Fraldi, D. L. Medina and A. Ballabio, *Nat. Rev. Mol. Cell Biol.*, 2013, **14**, 283; (*c*) M. E. Guicciardi, M. Leist and G. J. Gores, *Oncogene*, 2004, **23**, 2881; (*d*) H. B. Shi, R. T. K. Kwok, J. Z. Liu, B. G. Xing, B. Z. Tang and B. Liu, *J. Am. Chem. Soc.*, 2012, **134**, 17972.
3 (*a*) G. K. Tofaris, *Mov. Disord.*, 2012, **27**, 1364; (*b*) L. Bitensky, J. Chayen, G. J. Cunningham and J. Fine, *Nature*, 1963, **199**, 493.
4 (*a*) K. Glunde, C. A. Foss, T. Takagi, F. Wildes and Z. M. Bhujwalla, *Bioconjugate Chem.*, 2005, **16**, 843; (*b*) N. Fehrenbacher and M. Jäättelä, *Cancer Res.*, 2005, **65**, 2993.

5 (*a*) X. H. Wang, D. M. Nguyen, C. O. Yanez, L. Rodriguez, H. Y. Ahn, M. V. Bondar and K. D. Belfield, *J. Am. Chem. Soc.*, 2010, **132**, 12237; (*b*) L. Y. Yin, C. S. He, C. S. Huang, W. P. Zhu, X. Wang, Y. F. Xu and X. H. Qian, *Chem. Commun.*, 2012, **48**, 4486.
6 (*a*) H. Shi, X. X. He, Y. Yuan, K. M. Wang and D. Liu, *Anal. Chem.*, 2010, **82**, 2213; (*b*) S. Q. Wu, Z. Li, J. H. Han and S. F. Han, *Chem. Commun.*, 2011, **47**, 11276.
7 I. L. Medintz, H. T. Uyeda, E. R. Goldman and H. Mattoussi, *Nat. Mater.*, 2005, **4**, 435.
8 N. Bidère, H. K. Lorenzo, S. Carmona, M. Laforge, F. Harper, C. Dumont and A. Senik, *J. Biol. Chem.*, 2003, **278**, 31401.
9 S. Kawata and Y. Kawata, *Chem. Rev.*, 2000, **100**, 1777.
10 (*a*) G. Berkovic, V. Krongauz and V. Weiss, *Chem. Rev.*, 2000, **100**, 1741; (*b*) A. Setaro, P. Bluemmel, C. Maity, S. Hecht and S. Reich, *Adv. Funct. Mater.*, 2012, **22**, 2425; (*c*) F. A. Wang, X. Q. Liu and I. Willner, *Adv. Mater.*, 2013, **25**, 349.
11 (*a*) N. Shao, J. Y. Jin, S. M. Cheung, R. H. Yang, W. H. Chan and T. Mo, *Angew. Chem., Int. Ed.*, 2006, **45**, 4944; (*b*) J. Andersson, S. M. Li, P. Lincoln and J. Andréasson, *J. Am. Chem. Soc.*, 2008, **130**, 11836; (*c*) X. J. Xie, G. Mistlberger and E. Bakker, *J. Am. Chem. Soc.*, 2012, **134**, 16929.
12 (*a*) S. Silvi, A. Arduini, A. Pochini, A. Secchi, M. Tomasulo, F. M. Raymo, M. Baroncini and A. Credi, *J. Am. Chem. Soc.*, 2007, **129**, 13378; (*b*) V. Balzani, A. Credi and M. Venturi, *Chem. Soc. Rev.*, 2009, **38**, 1542.
13 (*a*) V. Balzani, A. Credi and M. Venturi, *ChemPhysChem*, 2003, **3**, 49; (*b*) D. B. Liu, W. W. Chen, K. Sun, K. Deng, W. Zhang, Z. Wang and X. Y. Jiang, *Angew. Chem., Int. Ed.*, 2011, **50**, 4103.
14 J. C. Wu, A. Zawistowski, M. Ehrmann, T. Yi and C. Schmuck, *J. Am. Chem. Soc.*, 2011, **133**, 9720.
15 T. Satoh, K. Sumaru, T. Takagi, K. Takai and T. Kanamori, *Phys. Chem. Chem. Phys.*, 2011, **13**, 7322.

